Non-Newtonian pulsatile blood flow in a modeled artery with a stenosis and an aneurysm

I. Husain , C. Langdon and J. Schwark
Department of Mathematics
Luther College – University of Regina
Regina, Saskatchewan
Canada S4S 0A2
Iqbal.Husain@uregina.ca http://www.uregina.ca

Abstract: - Mathematical modeling of blood flows in the arteries is an important and challenging problem. This study investigates the pulsatile simulations of blood flow through two three-dimensional models of an arterial stenosis and an aneurysm. Four non-Newtonian blood models, namely the Power Law , Casson, Carreau and the Generalized Power Law, as well as the Newtonian model of blood viscosity, are used to investigate the flow effects induced by these different blood constitutive equations. The aim of this study are three fold: firstly, to investigate the variation in wall shear stress in an artery with a stenosis or aneurysm at different flow rates and degrees of severity; secondly, to compare the various blood models and hence quantify the differences between the models and judge their significance and lastly, to determine whether the use of the Newtonian blood model is appropriate over a wide range of shear rates.

Key-Words: - fluid flows, blood, stenosis, aneurysm, non-newtonian, pulsatile, simulations.

1 Introduction

Since the hemodynamics hypotheses of artherosclerosis were first formulated several decades ago, flow imaging and computing have played an increasingly important role in advancing our understanding of how blood really flows in large arteries prone to atherosclerosis [1]. While lumped parameter and linear and nonlinear one-dimensional wave propagation methods received much attention in the 1950s through 1980s, computational fluid dynamics (CFD) methods based on solving the three dimensional equations of blood flow have had a dominant influence on current research efforts to quantify hemodynamic conditions in arteries.

The presence of a stenosis or an aneurysm in an artery may significantly alter the flow field and consequently the flow rate, leading to severe pathological incidences. In the case of a stenosis, the consequences may be cardiac arrest and stroke whereas the development of an aneurysm and its continuous dilation may lead to its rupture causing death or grave disability. Furthermore, the presence of the anomaly itself may produce flow disturbances such as vortex formation, which has been reported as a contributing factor to atherogenesis and thrombogenesis [2].

The aim of this study are three fold: firstly, to investigate the variation in wall shear stress in an artery with a stenosis or aneurysm at different flow rates and degrees of severity; secondly, to compare the various blood models and hence quantify the differences between the models and judge their significance and lastly, to determine whether the use of the Newtonian blood model is appropriate over a wide range of shear rates.

2. ANALYSIS AND MODELLING

Governing equations

The blood flow is assumed to be laminar and incompressible and therefore the Navier-Stokes equations for 3D incompressible flow are given by

$$\nabla \cdot V = 0 \tag{1}$$

$$\rho\left(\frac{\partial V}{\partial t} + V \,.\, \nabla V\right) = -\nabla . \tau - \nabla p \tag{2}$$

where V is the 3D velocity vector, p pressure, ρ density and τ the shear stress term.

Four different non-Newtonian blood flow models as well as the simple Newtonian model are considered in this study. The effects of these models on the flow field and the wall shear stress in the vicinity of a stenosis or aneurysm are examined. These models are given below [3].

Blood Models

1. Newtonian model

$$\mu = 0.00345 \quad Pa \cdot s \tag{3}$$

2. Power Law Model

$$\mu = \mu_0 (\dot{\gamma})^{n-1} \tag{4}$$

3. Casson Model

$$\mu = \frac{[\sqrt{\tau_y} + \sqrt{\eta |\dot{\gamma}|}]^2}{|\dot{\gamma}|} \tag{5}$$

4. Carreau Model

$$\mu = \mu_\infty + (\mu_0 - \mu_\infty)\left[1 + (\lambda\dot{\gamma})^2\right]^{(n-1)/2} \tag{6}$$

5. Generalized Power Law Model

$$\mu = \lambda |\dot{\gamma}|^{n-1} \tag{7}$$

where

$$\lambda(\dot{\gamma}) = \mu_\infty + \Delta\mu \exp\left[-\left(1 + \frac{|\dot{\gamma}|}{a}\right)\exp\left(\frac{-b}{|\dot{\gamma}|}\right)\right],$$

$$n(\dot{\gamma}) = n_\infty - \Delta n \exp\left[-\left(1 + \frac{|\dot{\gamma}|}{c}\right)\exp\left(\frac{-d}{|\dot{\gamma}|}\right)\right]$$

Geometry

The flow geometry comprises a tube of diameter D and can be divided into three regions, the inlet, the deformed and the outlet region. In the case of the stenosis, the lengths of these regions are $4D, 2D$ and $20D$, respectively. For the aneurysm, there are $4D, 4D$ and $18D$, respectively. The radius of the undeformed inlet and outlet is $R_0 = D/2$.

In the case of the stenosis, the radius of the constricted region is given by

$$R = R_0\left[1 - \left(\frac{R_0 - R_{\min}}{R_0}\right)\left(\frac{1 - \cos(2\pi x/D)}{2}\right)^2\right] \quad 0 \le x \le 2D \tag{8}$$

where $R_{\min}$ is the minimum radius at the centre of the stenosis. In this study, three different degrees of stenosis were used, 20%, 50% and 80%.

In the case of the aneurysm, the radius of the dilated region is given by

$$R = R_0 + (a - R_c + \sqrt{R_c^2 - (b/2 - x)^2}), \qquad 0 \le x \le b \tag{9}$$

where x is measured from the start of the dilated region, a is the maximum width of the dilated segment and

$$R_c = \frac{a^2 + (b/2)^2}{2a}$$

For this study, three different values of a 0.25, 0.4 and 0.55 were used.

Assumptions and boundary conditions

It is assumed that the arterial walls are rigid and no-slip condition is imposed at the walls. At the outlet, stress-free conditions are applied and the pressure is set to zero. Finally, the velocity profile at the inlet is regarded to be that of fully developed flow in a straight tube and can be derived analytically for both the Newtonian and the Power Law fluids [4]. The forms are

$$u = \bar{u}\left[1 - \left(\frac{r}{R_0}\right)^2\right] \qquad 0 \le r \le R_0 \tag{10}$$

where u is the velocity component in the $x-$ direction for the Newtonian flow and

$$u = \bar{u}\left(\frac{3n+1}{n+1}\right)\left[1 - \left(\frac{r}{R_0}\right)^{\frac{n+1}{n}}\right] \qquad 0 \le r \le R_0 \tag{11}$$

ISBN: 978-1-61804-110-4

for the non-Newtonian flow. In transient flow, the pulsatile flow at the inlet is given by a time varying forcing function given in [5]. This forcing function was scaled to yield a maximum inflow velocity of $\bar{u}$ with a heart rate of approximately 60 beats per minute.

Solution methodology

The governing equations are highly nonlinear and must be solved numerically using techniques of computational fluid dynamics. In this study, these equations are solved using the finite element method as implemented by COMSOL (COMSOL Inc., Los Angeles, CA). The flow geometries for the stenosis and aneurysm were first created using Matlab. Then a finite element mesh was placed on these geometries. Briefly, an inlet plane of the artery is meshed in 2D using triangles and this mesh is extruded along the centerline of the artery to create a 3D mesh consisting of hexadrel elements. The mesh used for all computations consisted of 9,708 elements and 15,048 nodes for the stenosis and 17,696 elements and 27,132 nodes for the aneurysm as shown in Figure 1.

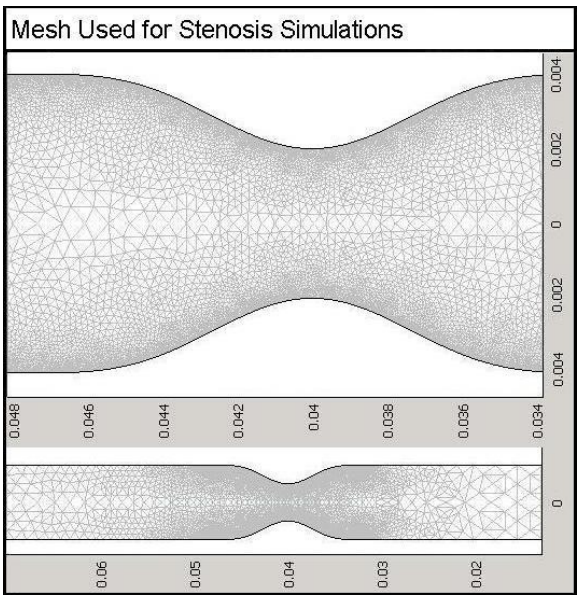

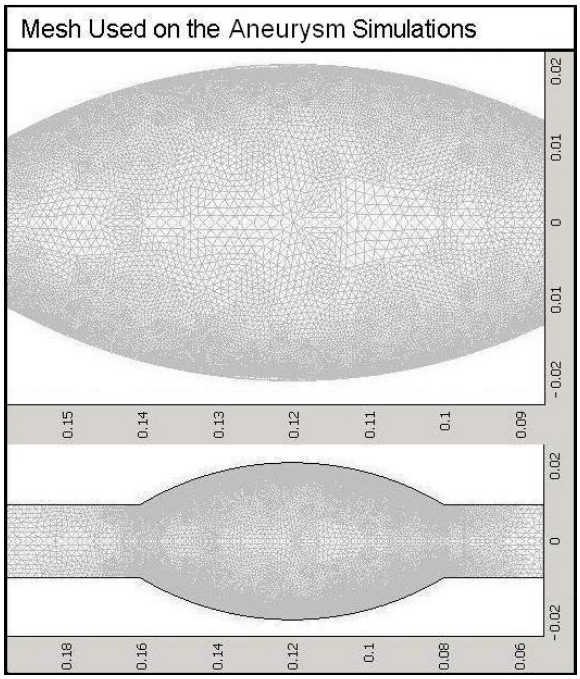

Figure 1 3D grid for stenosis and aneurysm

The governing equations were solved completely using the boundary conditions for fully developed flow (10) and (11) at the inlet along with the pulsatile forcing function for the transient case.

3. RESULTS AND DISCUSSION

Transient simulations were performed using all five models given above. Three different degrees of stenosis were used namely 20%, 50% and 80% and maximum dilated widths of 25%, 40% and 55% were examined for the aneurysm.

Figure 2 above shows that all of the non-Newtonian models considered here except the Power Law model produce a higher pressure difference than the Newtonian model. Specifically, the highest pressure drop is induced by the generalized Power Law model and the lowest by the Power Law model. Similar pattern in pressure differences are obtained at higher flow rates.

The distribution of the wall shear stress (WSS) is one of the most important hemodynamic parameter due to its direct relevance in artherosclerosis formation. Figure 3 shows the distributions of maximum shear stress for various degrees of severity of the stenosis for all models. It

ISBN: 978-1-61804-110-4

is evident that WSS increases with increasing severity. All models show close agreement with the Newtonian model except for the Power Law model. At 50% stenosis, the WSS predicted by this model is significantly lower than the rest. Figure 5 shows the distribution of WSS along the geometry at various times. Maximum shear stresses are reached just before the throat of the stenosis. The magnitude of this value increases with higher flow rates. This peak is followed by a negative value indicating the presence of backflow. Further downstream, the WSS steadily regains its undisturbed value.

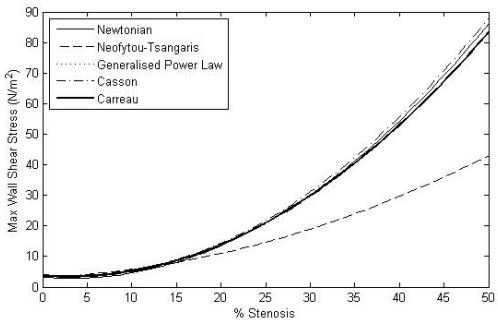

Figure 3
Wall Shear stress versus percent stenosis for various models, with 0.11196 m/s inflow rate.

The maximum WSS for various degrees of dilation of an aneurysm is displayed in Figure 4 for all models. There is less agreement between the models in this case. Only the Casson and the Carreau models are comparable throughout. The Power Law model gives a much lower $\tau_W^{\max}$ value because it exhibits a lower viscosity at the throat of the stenosis where the shear stress is high. As the flow rate increases, these WSS differences from various models become more prominent indicating significant differences in model behaviour.

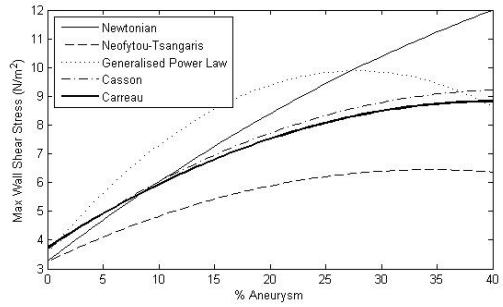

Figure 4
Wall shear stress versus percent dilation for various models, with 0.11196 m/s inflow rate.

Transient simulations were performed using the Generalized Power Law Model for both the stenosis and aneurysm. Each simulation was from $t = 0$ to 10.0 secs, yielding a heart rate of approximately 60 beats per minute.

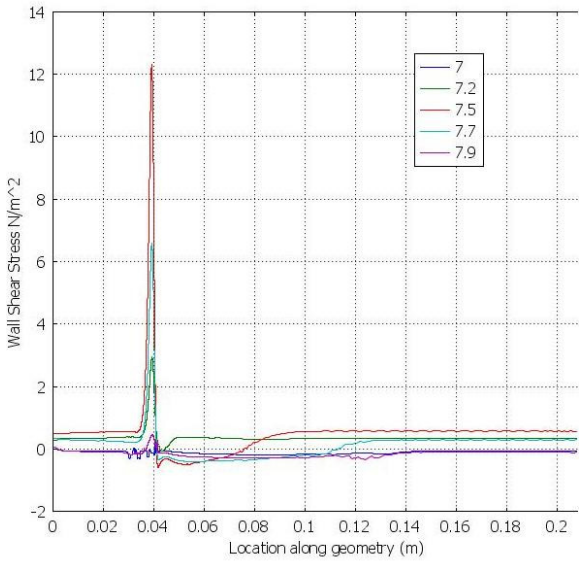

Figure 5
Wall shear stress for 50% stenosis pulsatile Generalized Power Law model at various time intervals, with 0.11196m/s max inflow rate

Figure 6 shows the distribution of maximum WSS with shear rate in a stenosis. Again, WSS increases with increasing shear rate with the Power Law model deviating significantly from the rest.

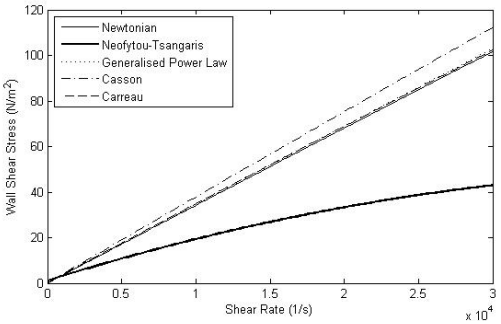

Figure 6

WSS versus shear rate in a stenosis

Figure 7 displays the maximum WSS for increasing shear rate in an aneurysm. There is less agreement between the models at higher shear rates with the Power law model showing the least agreement.

ISBN: 978-1-61804-110-4

The distribution of the WSS for the Generalized Power Law model is shown in Figure 8. The WSS drops as the flow enters the aneurysm and reaches a peak at the end of the dilated segment. This peak value increases with increasing flow rate. The negative WSS values indicate the presence of a recirculation region. As the flow exits the aneurysm, the WSS gradually regains its undisturbed value.

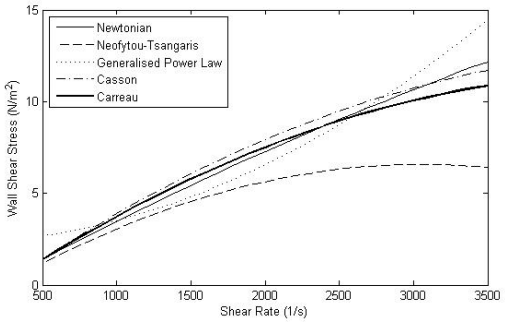

Figure 7
WSS versus shear rate in an aneurysm

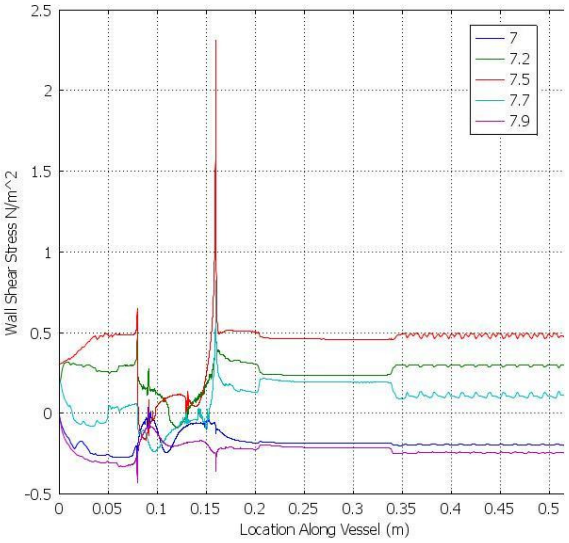

Figure 8
Wall shear stress for 55% aneurysm pulsatile Generalized Power Law model at various time intervals, with 0.13625 m/s max inflow rate

In the case of pulsatile flow through the aneurysm, the simulation was performed for 10 sec using the Generalized Power Law model. As in the case of the stenosis, results in Table 4 show the maximum WSS values are produced at mid-cycle corresponding to the peak inflow velocity. However, the maximum pressure is attained just before mid-cycle and the minimum pressure towards the end of the cycle. This maximum pressure is excessively high. It is not clear why this is so and further investigation is planned. The streamline patterns at various points of the cardiac cycle are shown in Figure 5. The formation and re-formation of the recirculation regions corresponding to the oscillatory nature of the pulsatile flow is evident.

The WSS distribution in pulsatile flow shown in Graph 6 display a similar pattern in mid-cycle as in the steady state case. The distribution at other times show some marked differences due to the development of backflow regions inside the aneurysm.

In all cases, for both the stenosis and the aneurysm, the flow field and the WSS changed significantly as the degree of abnormality increased. The recirculation regions become larger progressively and the WSS generally increases, especially for the stenosis.

4. CONCLUSIONS

A study of the effects of modeling blood flow through a stenosis and an aneurysm using five different blood rheological models is presented. The flow field and wall shear stress distributions produced by each model are investigated for various flow rates and degrees of abnormality. The results show that there are significant differences between simulating blood as a Newtonian or non- Newtonian fluid. It is found that the Newtonian model is a good approximation in regions of mid-range to high shear but the Generalized Power Law model provides a better approximation of wall shear stress at low shear.

These conclusions are presented under the assumption that the arterial walls are rigid and zero pressure is assumed at the outlet. A more realistic simulation would include elastic walls and incorporate the effects of upstream and downstream parts of the circulatory system into the boundary conditions. This is a long term objective of this study.

ISBN: 978-1-61804-110-4

References:

1. Berger, S.A. and Jou, L.-D., Flows in stenotic vessels, *Annual Reviews of Fluid Mechanics*, **32,** 2000, pp.347-382.
2. Ku, D.N., Blood flow in arteries, *Annual Review of Fluid Mechanics*, **29,** 1997, pp.399-434.
3. Johnston, B.M. et al., Non-Newtonian blood flow in human right coronary arteries: steady state simulations, *J. Biomechanics*, **37,** 2004, pp. 709-720.
4. Neofytou, P., and Tsangaris, S., Flow effects of blood constitutive equations in 3D models of vascular anomalies, *Int. J. Numer. Meth. Fluids*, **51,** 2005, pp. 489-510.